

A NEW METHOD OF DETERMINING THE INITIAL SIZE AND LORENTZ FACTOR OF GAMMA-RAY BURST FIREBALLS USING A THERMAL EMISSION COMPONENT

ASAF PE'ER¹, FELIX RYDE², RALPH A.M.J. WIJERS¹, PETER MÉSZÁROS³ AND MARTIN J. REES⁴

Draft version October 3, 2018

ABSTRACT

In recent years increasing evidence has emerged for a thermal component in the γ - and X-ray spectrum of the prompt emission phase in gamma-ray bursts. The temperature and flux of the thermal component show a characteristic break in the temporal behavior after a few seconds. We show here, that measurements of the temperature and flux of the thermal component at early times (before the break) allow the determination of the values of two of the least restricted fireball model parameters: the size at the base of the flow and the outflow bulk Lorentz factor. Relying on the thermal emission component only, this measurement is insensitive to the inherent uncertainties of previous estimates of the bulk motion Lorentz factor. We give specific examples of the use of this method: for GRB970828 at redshift $z = 0.9578$, we show that the physical size at the base of the flow is $r_0 = (2.9 \pm 1.8) \times 10^8 Y_0^{-3/2}$ cm and the Lorentz factor of the flow is $\Gamma = (305 \pm 28) Y_0^{1/4}$, and for GRB990510 at $z = 1.619$, $r_0 = (1.7 \pm 1.7) \times 10^8 Y_0^{-3/2}$ cm and $\Gamma = (384 \pm 71) Y_0^{1/4}$, where $Y = 1Y_0$ is the ratio between the total fireball energy and the energy emitted in γ -rays.

Subject headings: gamma rays: bursts — gamma rays: theory — plasmas — radiation mechanisms: non-thermal — radiation mechanisms: thermal

1. INTRODUCTION

In recent years increasing evidence has appeared that, during the first stages of the prompt emission of long duration gamma-ray bursts (GRBs), a thermal component accompanies the underlying non-thermal emission [Ryde (2004, 2005); Campana *et al.* (2006); see also Ghirlanda *et al.* (2003); Kaneko *et al.* (2003)].⁵ An analysis of BATSE bursts that are dominated by quasi-thermal emission (Ryde 2004, 2005) showed that the observed temperature exhibits a similar behavior in all of them: an initially (approximately) constant temperature at a canonical value $T_0^{ob.} \simeq 100$ keV which after $\sim 1 - 3$ seconds decreases as a power law in time $T^{ob.} \propto t^{-\alpha}$, with power law index $\alpha \simeq 0.6 - 1.1$. The redshifts of most of these bursts are unknown. An additional analysis (Ryde & Pe'er 2007) shows that after a short rise, the flux of the black body component of these bursts also decreases with time as $F_{BB}^{ob.} \propto t^{-\beta}$, with $\beta \simeq 2.0 - 2.5$. We showed there that this temporal behavior can be explained as due to the high latitude emission phenomenon (Fenimore *et al.* 1996; Granot *et al.* 1999; Qin 2002).

According to the standard fireball scenario, the non-thermal photons originate from the dissipation of the fireball kinetic energy. The dissipation mechanism (e.g., internal shocks (Paczynski & Xu 1994; Rees & Mészáros 1994), magnetic reconnection (Giannios & Spruit 2005;

Giannios 2006) or external shocks (Mészáros & Rees 1993; Dermer & Mitman 1999)) is yet uncertain, and can in principle occur at various locations. As opposed to this ambiguity in understanding the origin of the non-thermal component, the thermal component must originate at the photosphere. According to the high latitude emission interpretation of the data, the highest temperature and the maximal thermal flux initially observed are emitted from the photosphere on the radial axis towards the observer. Thus, in principle the radius of the emission site of these photons can be determined.

In this *Letter* we show that combined early time measurements of the observed temperature and thermal flux for bursts with known redshift allow us to directly determine the values of the bulk motion Lorentz factor, the physical size at the base of the flow and the photospheric radius. This is due to the fact that the observed temperature and flux of the thermal component depend on three internal parameters only: the isotropic equivalent luminosity of the thermal component L_{BB} , the Lorentz factor of the bulk motion of the flow at the photospheric radius η and the physical size at the base of the flow r_0 , and that L_{BB} can be directly measured for bursts with known redshift and measured thermal flux. In §2 we give a short description of the model, and implications are given in §3. In §4 we summarize and compare our results with those of previous methods of estimations of the bulk motion Lorentz factor.

2. MODEL: EXTENDED PHOTOSPHERIC EMISSION

In the classical fireball model of gamma-ray bursts (Goodman 1986; Paczyński 1986; Paczyński & Xu 1994), a thermal plasma of electrons, positrons, and photons expands rapidly from an initial radius r_0 . Conservation of energy and entropy imply that the bulk Lorentz factor of the flow increases as $\Gamma(r) \propto r$, until the plasma reaches the saturation radius $r_s = \eta r_0$, above which the

¹ Astronomical Institute “Anton Pannekoek”, Kruislaan 403, 1098SJ Amsterdam, the Netherlands; apeer@science.uva.nl

² Dept. of Physics, Royal Institute of Technology, AlbaNova, SE-106 91 Stockholm, Sweden

³ Dept. of Astron. & Astrophysics, Dept. of Physics, Pennsylvania State University, University Park, PA 16802

⁴ Institute of Astronomy, University of Cambridge, Madingley Rd., Cambridge CB3 0HA, UK

⁵ It was claimed by Ruffini *et al.* (2004); Bernardini *et al.* (2005) that afterglow emission can also be explained with a thermal component.

plasma Lorentz factor coasts with $\Gamma = \eta \equiv L/\dot{M}c^2$. Here, L is the isotropic equivalent burst luminosity, \dot{M} is the mass ejection rate and c is the speed of light (from here on we restrict the discussion to long bursts, characterized by extended emission of relativistic wind).

The photospheric radius r_{ph} is the radius above which the flow becomes optically thin to scattering by the baryon related electrons. Depending on the values of the free model parameters (η , L and r_0) this radius can be smaller or larger than r_s (Mészáros *et al.* 2002): for $\eta > (<) \eta_* \equiv (L\sigma_T/4\pi m_p c^3 r_0)^{1/4}$, $r_{ph} < (>) r_s$. Here, σ_T is the Thomson cross section and m_p is the proton mass. The luminosity L is measured for bursts with known redshift, $L = 4\pi d_L^2 Y F^{ob}$, where d_L is the luminosity distance, F^{ob} is the total (thermal + non thermal) observed γ -ray flux, and $Y \equiv \epsilon/\epsilon_\gamma \geq 1$ is the ratio between the total fireball energy and the energy emitted in γ -rays. As we show below, the measurement of r_0 is similar in both scenarios, $r_{ph} > (<) r_s$. Thus, it is possible to determine whether r_{ph} is below or above r_s from measurable quantities, and to determine η in the second case.

The thermal component originates from the photosphere of an expanding plasma jet. The observed thermal flux (integrated over all frequencies) is given by integrating the intensity over the emitting surface, $F_{BB}^{ob} = (2\pi/d_L^2) \int d\mu \mu r_{ph}^2 \mathcal{D}^4 (\sigma T'^4/\pi)$. Here, T' is the comoving temperature at the photospheric radius, σ is Stefan's constant and $\mathcal{D} = \mathcal{D}(\theta)$ is the Doppler factor, $\mathcal{D} = [\Gamma(1 - \beta\mu)]^{-1}$. The angle θ is the angle between the direction of the outflow velocity vector (β) and the line of sight, $\mu \equiv \cos(\theta)$, and $\Gamma = (1 - \beta^2)^{-1/2}$ is the outflow Lorentz factor. For a plasma Lorentz factor much larger than the inverse of the jet opening angle $\Gamma \gg \theta_j^{-1}$ and for early enough times, at a given observed time the integration boundaries are determined uniquely by the emission duration, regardless of the value of θ_j .

Due to the Doppler effect and to the cosmological redshift, photons that are emitted at frequency ν' in the comoving frame of a relativistically expanding plasma with Lorentz factor Γ at redshift z , are observed at frequency $\nu^{ob} = \mathcal{D}(\theta)\nu'/(1+z)$. For $\Gamma \gg 1$ and emission on the line of sight, $\nu^{ob} \simeq 2\Gamma\nu'/(1+z)$. In the extended emission interpretation of the data (Ryde & Pe'er 2007), an observer sees simultaneously photons that originate from a range of angles to the line of sight, $\theta_{\min} \leq \theta \leq \theta_{\max}$. In this case, a thermal spectrum (with temperature T') in the comoving frame is observed as a modified black-body spectrum. Nonetheless, the observed spectrum is very similar to a pure black-body spectrum (Pe'er 2007).

During the first few seconds, when the observed temperature is nearly constant, the observed radiation is dominated by photons emitted close to the line of sight, i.e., $\theta_{\min} = 0$. According to this interpretation, at $t^{ob} > t_{break}$, there is no more emission from $\theta = 0$ because the inner engine activity decreases, and the emission is dominated by high latitude effects. Here, t_{break} is the break time in the temperature's temporal behavior. At $t^{ob} < t_{break}$, the observed spectrum is very close to a black body spectrum with temperature $T^{ob} \simeq 1.48\Gamma T'/(1+z)$ (Pe'er 2007)⁶. During this pe-

riod, the upper integration boundary in the equation for the thermal flux is $\mu_{\max} = \cos(\theta_{\min}) = 1$, and the ratio $(F_{BB}^{ob}/\sigma T^{ob.4})^{1/2}$ which we denote as \mathcal{R} , is equal to

$$\mathcal{R} \equiv \left(\frac{F_{BB}^{ob}}{\sigma T^{ob.4}} \right)^{1/2} = (1.06) \frac{(1+z)^2 r_{ph}}{d_L \Gamma}. \quad (1)$$

The prefactor (1.06) originates from the dependence of the photospheric radius on the angle to the line of sight (Pe'er 2007).

We can now make the discrimination between the two possible cases: $r_{ph} < (>) r_s$. If $r_{ph} < r_s$, then $\Gamma(r) \propto r$. In this case, $r_{ph}/\Gamma = r_0$, and equation 1 becomes

$$r_0(r_{ph} < r_s) = \frac{1}{(1.06)} \frac{d_L}{(1+z)^2} \mathcal{R}. \quad (2)$$

In this case, it is not possible to determine the photospheric radius, or the value of $\Gamma(r_{ph})$.

In the case $r_{ph} > r_s$, the photospheric radius is given by $r_{ph} = (L\sigma_T/8\pi\eta^3 m_p c^3)$ (Mészáros *et al.* 2002; Daigne & Mochkovitch 2002; Broderick 2005). At this radius, the comoving temperature is given by

$$T'(r_{ph}) = \left(\frac{L}{4\pi r_0^2 ca} \right)^{1/4} \eta^{-1} \left(\frac{r_{ph}}{r_s} \right)^{-2/3}, \quad (3)$$

where a is the radiation constant. Setting $\Gamma = \eta$ and $L = 4\pi d_L^2 Y F^{ob}$ in the equation of the photospheric radius, one obtains from equation 1 the coasting value of the Lorentz factor,

$$\eta = \left[(1.06)(1+z)^2 d_L \frac{Y F^{ob} \sigma_T}{2m_p c^3 \mathcal{R}} \right]^{1/4}. \quad (4)$$

Equations 1, 3 and 4 now give the physical size at the base of the flow,

$$r_0(r_{ph} > r_s) = \frac{4^{3/2}}{(1.48)^6 (1.06)^4} \frac{d_L}{(1+z)^2} \left(\frac{F_{BB}^{ob}}{Y F^{ob}} \right)^{3/2} \mathcal{R}. \quad (5)$$

We thus find that a measurement of \mathcal{R} and the ratio of the black body flux to the total flux at the very early observed times from bursts with known redshift give a direct measurement of r_0 , and that the result is similar (up to a numerical factor of the order unity, provided that Y is not much larger than 1; see discussion on the value of Y in §4), for the two considered cases, $r_{ph} < (>) r_s$. The measured values of r_0 and L can be used to determine the value of η_* , which is independent of the specific scenario. One can then use the measured values of \mathcal{R} and F^{ob} to determine the value of η using equation 4. If the obtained value is larger than the value of η_* , then $r_{ph} < r_s$, in which case equation 4 should not be used and the value of η remains undetermined.

3. IMPLICATIONS

Relations 4 and 5 allow a direct measurement of the size at the base of the flow, r_0 and of the bulk motion Lorentz factor of the flow from GRBs with known redshift and energy content. In addition, it is possible to

erature as $T^{ob} \simeq \Gamma T'/(1+z)$. In fact, $\mathcal{D}(\theta = 1) \simeq 2\Gamma$, thus one should add an extra factor of 2. The factor 1.48 used here results from the angular integration. See Pe'er (2007) for details.

⁶ The relation between T^{ob} and T' is often written in the lit-

determine the photospheric radius r_{ph} and the saturation radius r_s , if measurements of the thermal flux and temperature are available at early enough times.

We illustrate the use of this method on two bursts with known redshifts, namely GRB970828 and GRB990510 observed by the BATSE detectors aboard the *Compton Gamma Ray Observatory*. BATSE detected bursts in the 20 keV – 2 MeV energy range. The time-resolved spectra for the selected bursts were fitted using a Planck function and a single power-law to model the photospheric and the non-thermal emission components, following the method presented in Ryde (2004) (see also Ryde & Pe’er 2007).

The analysis of the thermal component of GRB970828 is presented in figures 1. This burst, at redshift $z = 0.9578$, had a good temporal coverage for the first 100 seconds. The left hand panel in Figure 1 shows the temporal behavior of the temperature of the thermal component. During the first ~ 8 seconds the observed temperature rises slightly to a value of 78.5 keV, after which it shows a rapid decrease that can be fitted as a power law in time with a power law index $\alpha = -0.51$. In the right hand panel of Figure 1 we show the temporal behavior of the function \mathcal{R} . This function shows a slight increase during the first ~ 7 seconds, after which it rises as a power law in time with a power law index $\beta = 0.67$. The smooth increase of \mathcal{R} before the break implies that there is no significant energy dissipation below the photosphere, which, if it occurred would result in a strong fluctuation and affect the smoothness of \mathcal{R} . The break times in the temporal behavior of the observed temperature and \mathcal{R} are the same within the errors.

According to the extended high latitude emission interpretation of this result, we deduce that the first episode of significant inner engine activity took place during the first 7 – 8 seconds, and at later times we are observing photons emitted off axis (we neglect here late time episodes of engine activity that occur after ~ 25 s and ~ 60 s in this burst). The values of r_0 and η are calculated using the observed values of the temperature $T^{ob.} = 78.5 \pm 4.0$ keV, $\mathcal{R} = (1.88 \pm 0.28) \times 10^{-19}$, and the ratio of thermal to total flux $F_{BB}^{ob.}/F^{ob.} = 0.64 \pm 0.20$ at the break time. The error bars on the measured quantities are averaged over the first seconds, before the temporal break. Considering a flat universe with $\Omega_\Lambda = 0.73$, $H_0 = 71$ km/s/Mpc, the luminosity distance for this burst is $d_L = 1.94 \times 10^{28}$ cm. Using equations 4 and 5, we find that $\Gamma = (305 \pm 28) Y_0^{1/4}$ and $r_0 = (2.9 \pm 1.8) \times 10^8 Y_0^{-3/2}$ cm, where $Y = 1 Y_0$. The calculated value of $\eta_* = 463 Y_0^{5/8}$ proves that indeed $r_{ph} = 2.7 \times 10^{11} Y_0^{1/4}$ cm is larger than $r_s = 9.0 \times 10^{10} Y_0^{-5/4}$ cm, which implies that $\eta = \Gamma = 305 Y_0^{1/4}$ is the coasting value of the outflow Lorentz factor. The statistical error on the estimated value of η is $\lesssim 10\%$. The systematical error results from the uncertainty in the value of Y , and is not expected to be more than tens of percents (see §4 below), giving the best constraint on the estimated value of η measured so far.

A similar analysis was carried out for GRB990510 at $z = 1.619$. The results obtained are similar, $r_0 = (1.7 \pm 1.7) \times 10^8 Y_0^{-3/2}$ cm and $\eta = (384 \pm 71) Y_0^{1/4}$. The larger statistical errors compared to GRB970828 mainly

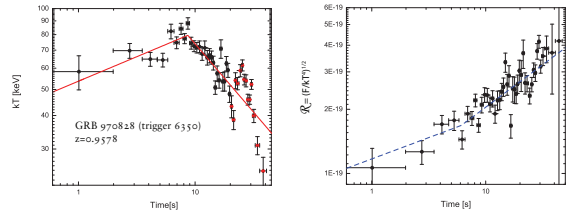


FIG. 1.— Temporal behavior of the thermal component in GRB970828 at $z = 0.9578$. Left panel: the observed temperature. During the first ~ 8 s the temperature rises slowly up to 78.5 keV, after which it decreases as a power law in time with power law index -0.51 . The fit was made on the data up to 20 s, which includes the first pulse structure of the light curve. Right panel: the temporal behavior of the ratio $\mathcal{R} \equiv (F_{BB}/\sigma T^{ob4})^{1/2}$. This ratio increases slowly during the first ~ 7 s, after which it increases as a power law in time with power law index 0.67. The break time after ~ 7 s is close to the break time in the temporal behavior of the temperature.

reflect the fewer available data points for this burst. The value of $\eta_* = 830 Y_0^{5/8}$ proves that indeed $r_{ph} = 7.7 \times 10^{11} Y_0^{1/4}$ cm is larger than $r_s = 6.3 \times 10^{10} Y_0^{-5/4}$. The temporal behavior of the observed temperature and \mathcal{R} were found to be similar in a large sample of BATSE bursts, providing further evidence for our model. However, the redshift of most of these bursts is unknown, thus definite values of η and r_0 could not be obtained. The full sample appears in Ryde & Pe’er (2007).

4. DISCUSSION

In this *Letter* we showed that by measuring the observed temperature and thermal flux of the thermal component that accompanies the prompt emission of GRBs, it is possible to determine the values of two of the least restricted parameters of the fireball model: the size at the base of the flow and the outflow bulk Lorentz factor (in the case that the photospheric radius is larger than the saturation radius). In this case, it is also possible to determine the saturation radius r_s and the photospheric radius r_{ph} . We showed that the calculation of the initial size of the flow (equations 2, 5) is similar (up to a constant of the order unity) for the cases $r_{ph} > (<) r_s$. This allows a comparison between the measured value of η (equation 4) and the derived value of η_* , and a discrimination between the two cases. We have given examples of the use of this method for the determination of η and r_0 for two specific GRBs.

The largest uncertainty in the estimate of η is due to the uncertainty in the value Y . Value of $1 \lesssim Y < 3 - 5$ were suggested based on afterglow observations (Freedman & Waxman 2001; Frail *et al.* 2001; Friedman & Bloom 2005; Granot *et al.* 2006). Theoretical arguments based on fitting the flux of ultra-high energy cosmic rays (UHECR; Wick *et al.* 2004), under the assumption that UHECRs originate from GRBs (Waxman 1995; Vietri 1995), as well as efficiency considerations (Fan & Piran 2006) suggest larger value, $Y \gtrsim 10$. For bursts with a dominant thermal component, as considered here, we expect Y to be close to unity. If afterglow measurements of bursts with detected thermal component and known redshift become available, as expected after the launch of the *GLAST* satellite, this uncertainty could be removed. A second source of systematic uncertainty can result from dominating Compton scattering (which conserves the number

of photons) resulting in a Wien spectrum, rather than a thermal spectrum. Observationally, a Wien spectrum is hard to discriminate from a thermal spectrum. In this case, the systematic error in estimating the temperature is $(3k_B T)/(2.7k_B T) \sim 10\%$, which transforms into $\sim 5\%$ uncertainty in the estimated value of η . Currently, this uncertainty is smaller than the statistical uncertainty, $\gtrsim 10\%$.

Other methods of estimating the bulk motion Lorentz factor in GRBs relied on a large number of uncertain model assumptions and uncertainties in the values of the free model parameters. A widely used lower limit for η is obtained by calculating the minimum Lorentz factor required in order for the observed energetic photons not to annihilate (Krolik & Pier 1991; Fenimore *et al.* 1993; Woods & Loeb 1995; Baring & Harding 1997; Lithwick & Sari 2001). In addition to providing only a lower limit, in order to get a good estimate of η_{\min} a wide spectral coverage of the GRB emission, from the optical band to the γ -rays is required. In these calculations, the prompt emission spectrum is sometimes approximated as a broken power law (e.g., Lithwick & Sari 2001), which may be too simplified (e.g., Pe'er & Waxman 2004).

An alternative method to estimate the Lorentz factor is by modeling the early afterglow emission, on the assumption that the optical flash observed in a few cases results from synchrotron emission by electrons heated by the reverse shock (Sari & Piran 1999). A serious drawback of this method is that the estimate relies on the poorly known shock microphysics parameters (such as ϵ_e , ϵ_B etc.). A more advanced method, introduced by Zhang *et al.* (2003), relies on comparing the emission from the forward and reverse shock during the early afterglow. An underlying assumption in this estimate is that the values of the microphysics parameters at the forward and the reverse shocks are similar. Other methods rely on measurements of the physical parameters during the late afterglow emission, assuming that the flow expands in a self-similar motion during this phase. The initial value of the Lorentz factor is deduced by measuring the rise time of the early afterglow (Sari 1999; Wang *et al.* 2000; Soderberg & Ramirez-ruiz 2002; Kobayashi & Zhang 2003). An inherent drawback of this method is the assumption that the microphysical parameters are constant

in time during the late afterglow.

The method presented here of estimating η is independent of any of the uncertainties inherent in the former methods. Moreover, it gives a direct measurement of η , rather than a lower limit. The results presented in §3 (see also Ryde & Pe'er 2007) indicate values of η close to the earlier estimates. In addition, the values found for the size at the base of the flow r_0 could further constrain GRB progenitor models. The statistical errors on the values of these numbers are much smaller than any previous estimates.

These facts have several important consequences. First, they strengthen the interpretation of the prompt emission as being composed of a thermal component, in addition to the non-thermal component. Therefore, any interpretation of the prompt emission data must take this thermal component into account. Second, it shows that the extended high latitude emission interpretation of the late time temporal behavior of the thermal component is consistent with the fireball model predictions. Thus, this interpretation may also be used to understand the strong X-ray flares observed by the *SWIFT* satellite. Third, the consistency found between the different methods for estimating the value of η can be used to strengthen the validity of the underlying assumptions in previous estimates of η , such that the values of the microphysical parameters (ϵ_e , ϵ_B , etc.) are indeed constant in time during the afterglow emission phase. And last, the direct measurement of the physical size at the base of the flow is another, independent indication that a massive star is indeed the progenitor of long duration GRBs. Since η is related to the mass ejection rate, our measurements could be useful to constrain models of GRB progenitors.

This research was supported by NWO grant 639.043.302 to R.W.. F.R. acknowledges the support by the Swedish National Space Board. P.M. wishes to acknowledge the support by NASA NAG5-13286 and NSF AST0307376. This research made use of data obtained through the HEASARC Online Service provided by the NASA Goddard Space Flight Center. F.R. wishes to express his gratitude to the Department of Astronomy at Amsterdam University for their hospitality. We wish to thank the anonymous referee for useful comments.

REFERENCES

- Baring, M.G., & Harding, A.K. 1997, ApJ, 491, 663
 Bernardini, M.G., *et al.* 2005, ApJ, 634, L29
 Broderick, A.E. 2005, MNRAS, 361, 955
 Campana, S., *et al.* 2006, Nature, 442, 1008
 Daigne, F., & Mochkovitch, R. 2002, MNRAS, 336, 1271
 Dermer, C.D., & Mitman, K.E. 1999, ApJ, 513, L5
 Fan, Y., & Piran, T. 2006, MNRAS, 369, 197
 Fenimore, E.E., Epstein, R.I., & Ho, C. 1993, A&A, 97, 59
 Fenimore, E.E., Madras, C.D., & Nayakshin, S. 1996, ApJ, 473, 998
 Frail, D.A., *et al.* 2001, ApJ, 562, L55
 Freedman, D.L., & Waxman, E. 2001, ApJ, 547, 922
 Friedman, A.S., & Bloom, J.S. 2005, ApJ, 627, 1
 Giannios, D. A&A 457, 763
 Giannios, D., & Spruit, H.C. A&A 430, 1
 Ghirlanda, G., Celotti, A., & Ghisellini, G. 2003, A&A, 406, 879
 Goodman, J. 1986, ApJ, 308, L43
 Granot, J., Piran, T., & Sari, R. 1999, ApJ, 513, 679
 Granot, J., Königl, A., & Piran, T. 2006, MNRAS, 370, 1946
 Kaneko, Y., Preece, R.D., & Briggs, M.S. 2003, AAS meeting, 203, 80.04
 Kobayashi, S., & Zhang, B. 2003, ApJ, 597, 455
 Krolik, J. H., & Pier, E.A. 1991, ApJ, 373, 277
 Lithwick, Y., & Sari, R. 2001, ApJ, 555, 540
 Mészáros, P., & Rees, M.J. 1993, ApJ, 405, 278
 Mészáros, P., *et al.* 2002, ApJ, 578, 812
 Paczyński, B. 1986, ApJ, 308, L43
 Paczyński, B., & Xu, G. 1994, ApJ, 427, 708
 Pe'er, A. 2007, (in preparation)
 Pe'er, A., & Waxman, E. 2004, ApJ, 613, 448
 Qin, Y.-P. 2002, A&A, 396, 705
 Rees, M.J., & Mészáros, P. 1994, ApJ, 430, L93
 Ruffini, R., *et al.* 2004, Int.J.Mod.Phys.D, 13, 843
 Ryde, F. 2004, ApJ, 614, 827
 Ryde, F. 2005, ApJ, 625, L95
 Ryde, F., & Pe'er, A. 2007, in preparation
 Sari, R. 1999, A&AS, 138, 537
 Sari, R., & Piran, T. 1999, ApJ, 517, L109
 Soderberg, A.M., & Ramirez-Ruiz, E. 2002, MNRAS, 330, L24

- Vietri, M. 1995, ApJ, 453, 883
Wang, X.Y., Dai, Z.G. & Lu, T. 2000, MNRAS, 319, 1159
Waxman, E. 1997, Phys. Rev. Lett., 75, 386
Wick, S.D., Dermer, C.D., & Atoyan, A. 2004, Astropart. Phys., 21, 125
- Woods, E., & Loeb, A. 1995, ApJ, 453, 583
Zhang, B., Kobayashi, S. & Mészáros, P. 2003, ApJ, 595, 950